

This allows a comparison of temperature-standardized resting metabolic rates with Hemmingsen's classical study (1) (Fig. 4). Hemmingsen's work implies that ectotherms, endotherms, and unicells have distinctively different, nonoverlapping metabolic allometries. He argues that this suggests three major steps in the evolution of animal metabolism. The data in Fig. 4 show that this is an oversimplification. Temperature-standardized metabolic rates do not differ among unicells, invertebrates, and plants, but the rates for ectothermic vertebrates (fishes, amphibians, and reptiles) are slightly higher, and the rates for endothermic birds and mammals are slightly higher still. So instead of these groups having no overlap and differing by a factor of approximately 225 as suggested by Hemmingsen, there is extensive overlap with the average metabolic rates of unicells and plants separated from those of birds and mammals by about 20-fold.

Thus, metabolic rate—the rate at which organisms transform energy and materials—is governed largely by two interacting processes: the Boltzmann factor, which describes the temperature dependence of biochemical processes, and the quarter-power allometric relation, which describes how biological rate processes scale with body size. Here we show that using  $Q_{10}$  can introduce substantial error and that the temperature dependence of metabolic rate is relatively constant across a range of temperatures from 0 to 40°C. Application of the UTD to data on biological rate processes should reveal when the observed variation in response to temperature can be explained parsimoniously by Eq. 1, and when some additional biological mechanism is required. Emphasis on how metabolic rates depend primarily on body size and temperature promises to contribute to understanding how microbes, plants, and animals control the fluxes and storage of energy and materials on scales from local ecosystems to the biosphere (13, 14).

References and Notes

1. A. M. Hemmingsen, *Rep. Steno Mem. Hosp. and Nordisk Insulin Laboratorium* **9**, 6 (1960).
2. M. Kleiber, *Hilgardia* **6**, 315 (1932).
3. G. B. West, B. J. Enquist, J. H. Brown, *Nature* **398**, 573 (1998).
4. G. B. West, J. H. Brown, B. J. Enquist, *Science* **276**, 122 (1997).
5. R. A. H. Vetter, *J. Comp. Physiol. B* **165**, 46 (1995).
6. J. A. Raven, R. J. Geider, *New Phytol.* **110**, 441 (1988).
7. Metabolic rates were measured as resting rates using oxygen consumption in animals and unicells, and oxygen consumption or carbon dioxide production in plants. A respiratory coefficient of 1 was used to convert CO<sub>2</sub> production to O<sub>2</sub> consumption in plants. A density of 1.43 g/l for O<sub>2</sub> and 1.97 g/l for CO<sub>2</sub> was used to convert various units to ml/hour. A factor of 0.335 W/g was used to convert ml/hour to W/g<sup>3/4</sup>. Unicell mass was sometimes estimated from volume using a density of 1 g/ml. Metabolic rates of fish were stipulated as standard rates. Sources for all data presented in this paper, and statistics for regressions presented in Web fig. 1 and table 1 are available on

Science Online at [www.sciencemag.org/cgi/content/full/293/5538/2248/DC1](http://www.sciencemag.org/cgi/content/full/293/5538/2248/DC1).

8. K. A. Nagy, *Ecol. Monogr.* **57**, 111 (1987).
9. A. J. Hulbert, P. L. Lewis, *Annu. Rev. Physiol.* **62**, 207 (2000).
10. K. J. Niklas, B. J. Enquist, *Proc. Natl. Acad. Sci. U.S.A.* **98**, 2922 (2001).
11. F. Geizer, *J. Comp. Physiol. B* **158**, 25 (1988).
12. Metabolic rates in Fig. 4 were standardized to 20°C using the equation:  $B/M_{20C} = B/M_t e^{\alpha(1/20-1/t)}$  where  $t$  is body temperature and  $\alpha$  is the slope of the line for each species group from Fig. 1.

13. R. B. Rivken, L. Legendre, *Science*, **291**, 2398 (2001).
14. R. Valentini *et al.*, *Nature*, **404**, 861 (2000).
15. J.F.G., G.B.W., and J.H.B. are grateful for the support of the Thaw Charitable Trust and a Packard Interdisciplinary Science Grant; V.M.S., for the support of the National Science Foundation; and E.L.C., for the support received as a MacArthur Fellow. All are grateful to William Woodruff for discussions. Lastly, J.F.G. acknowledges the support and encouragement received from R. J. Gillooly.

25 April 2001; accepted 1 August 2001

## A Circadian Output in *Drosophila* Mediated by Neurofibromatosis-1 and Ras/MAPK

Julie A. Williams,<sup>1,2</sup> Henry S. Su,<sup>1,2</sup> Andre Bernards,<sup>4</sup> Jeffrey Field,<sup>3</sup> Amita Sehgal<sup>1,2\*</sup>

Output from the circadian clock controls rhythmic behavior through poorly understood mechanisms. In *Drosophila*, null mutations of the neurofibromatosis-1 (*Nf1*) gene produce abnormalities of circadian rhythms in locomotor activity. Mutant flies show normal oscillations of the clock genes *period* (*per*) and *timeless* (*tim*) and of their corresponding proteins, but altered oscillations and levels of a clock-controlled reporter. Mitogen-activated protein kinase (MAPK) activity is increased in *Nf1* mutants, and the circadian phenotype is rescued by loss-of-function mutations in the Ras/MAPK pathway. Thus, *Nf1* signals through Ras/MAPK in *Drosophila*. Immunohistochemical staining revealed a circadian oscillation of phospho-MAPK in the vicinity of nerve terminals containing pigment-dispersing factor (PDF), a secreted output from clock cells, suggesting a coupling of PDF to Ras/MAPK signaling.

The endogenous circadian pacemaker controls the daily oscillations of both cellular and behavioral processes and can be entrained to environmental cues such as light and maintain daily cycling in the absence of such cues. The molecular components of the circadian clock form a perpetually oscillating 24-hour feedback loop (1). The signaling mechanism that mediates output from these clock proteins to behavior is not known, although a secreted neuropeptide, PDF, may be a crucial output element in *Drosophila* (2).

We sought to identify other output signaling components by testing candidate molecules. One of these, the neurofibromatosis-1 (*Nf1*) gene product neurofibromin, is highly conserved between humans and flies, with sequence similarity throughout the length of the protein (3). In humans, *Nf1* is a tumor suppressor. Neurofibromin inactivates the Ras onco-

gene through hydrolysis of guanosine triphosphate (GTP) (4) and lack of neurofibromin expression in humans causes neurofibromatosis type 1 (NF-1). *Nf1*-deficient flies share some phenotypes with the human counterpart: Mutant flies are small (5), and short stature is a feature of some NF-1 patients (5). *Nf1* humans, flies, and mice all show learning deficits (5–7). The *Drosophila* neurofibromin can act as a Ras-GTPase activating protein in vitro (3), but no links to Ras have been demonstrated in vivo. Instead, all defects associated with mutations of the *Nf1* gene in flies are rescued by up-regulation of cyclic adenosine 3',5'-monophosphate (cAMP)-dependent signaling. Because other defects in cAMP signaling have resulted in circadian phenotypes (8–10), we hypothesized that *Nf1* mutants would also exhibit abnormal circadian behavior.

To determine the effect of *Nf1* on circadian rhythms, locomotor activity in constant darkness (DD) was monitored in adult flies carrying a null mutation in the *Nf1* gene either by deletion (*Nf1<sup>P1</sup>*) or by P-element insertion (*Nf1<sup>P2</sup>*) (3). None of the *Nf1<sup>P1</sup>* flies were rhythmic [see (11)], and only 10% of *Nf1<sup>P2</sup>* flies displayed weak rhythms (Table 1). The parental strain, *K33*, which contains a

<sup>1</sup>Howard Hughes Medical Institute, <sup>2</sup>Center for Sleep and Respiratory Neurobiology, <sup>3</sup>Department of Pharmacology, University of Pennsylvania School of Medicine, Philadelphia, PA 19104, USA. <sup>4</sup>Massachusetts General Hospital Cancer Center, Charlestown, MA 02129, USA.

\*To whom correspondence should be addressed. E-mail: [amita@mail.med.upenn.edu](mailto:amita@mail.med.upenn.edu)

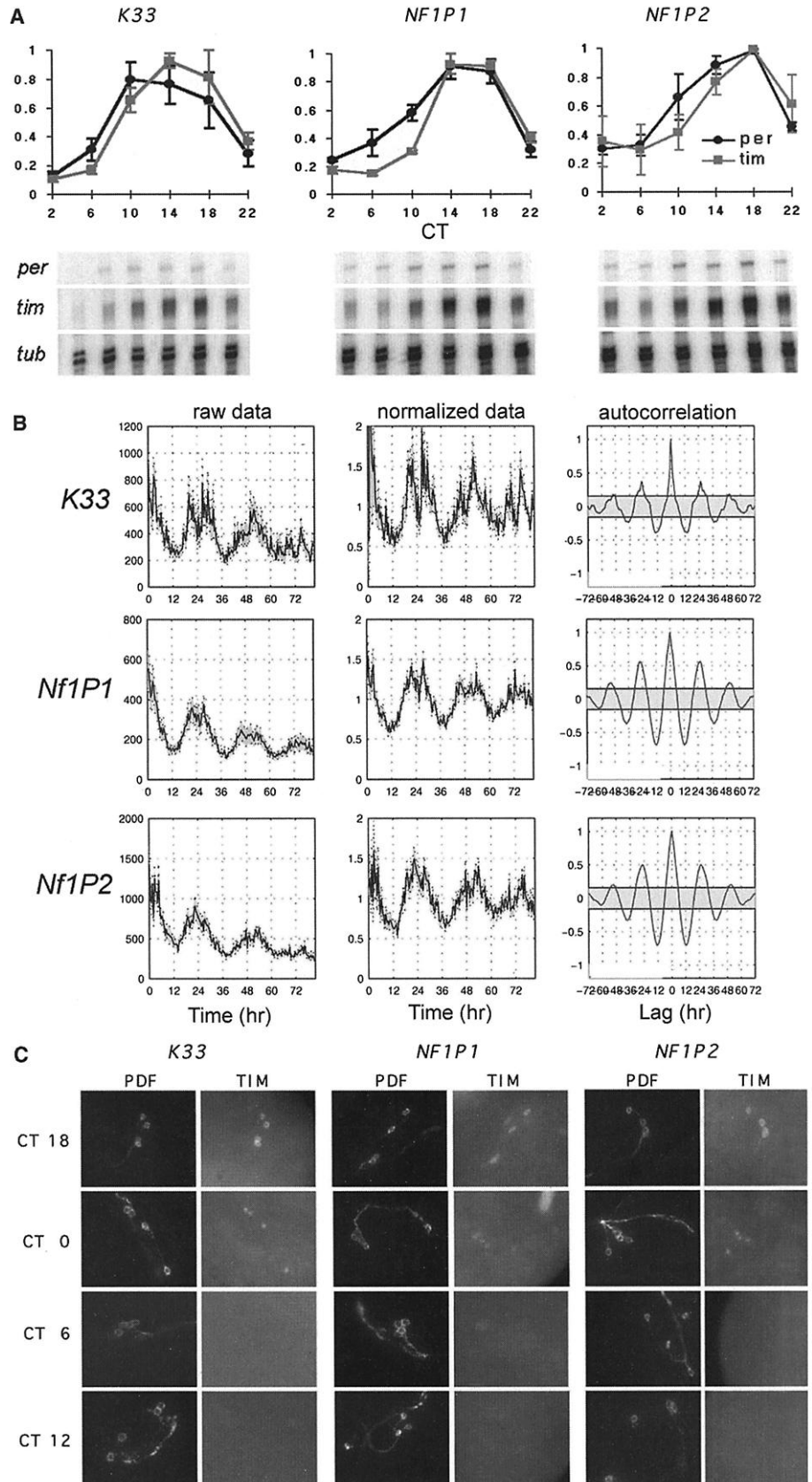
## REPORTS

P-element insertion that has no effect on *Nf1* expression, exhibited wild-type behavior (greater than 95% of the flies were rhythmic). The mutation did not affect adult flies' general

locomotor ability. No significant differences in activity counts were observed between each of the genotypes in DD at 25°C (*K33*,  $1027.35 \pm 80.0$  average activity counts per

day,  $n = 21$  flies; *Nf1<sup>P1</sup>*,  $1223.88 \pm 98.81$ ,  $n = 21$ ; and *Nf1<sup>P2</sup>*,  $1354.90 \pm 164.69$ ,  $n = 16$ ;  $P > 0.05$ , Student's *t* test), indicating that the effect of the *Nf1* mutations is on the

**Fig. 1.** Effects of *Nf1* on circadian clock genes. **(A)** RNase protection assays (RPAs) were performed to measure the abundance of *per* and *tim* mRNA relative to a control, *tubulin* (*tub*), at various time points in constant darkness. Data are the means  $\pm$  SEM of normalized data from three independent experiments. Representative RPAs are shown below each panel (11). **(B)** TIM-luc reporter activity in *K33* ( $n = 14$ ), *Nf1<sup>P1</sup>* ( $n = 23$ ), and *Nf1<sup>P2</sup>* ( $n = 15$ ) flies. Raw data were averaged across flies and plotted in the left panels (shaded area, SEM). Data were detrended and normalized to remove both linear and nonlinear trends (29) resulting from depletion of the luciferin substrate (middle panels). Autocorrelation analyses of the normalized data (right panels) indicate significant circadian oscillations for all three genotypes (95% confidence is indicated by shaded area centered around 0). **(C)** Whole mounts of larval brains from *K33*, *Nf1<sup>P1</sup>*, and *Nf1<sup>P2</sup>* flies were double-labeled for TIM and PDF (11). The left panels for each genotype show staining for PDF. The right panels correspond to the same field under a different wavelength to show the staining for TIM.



## REPORTS

behavioral rhythm and not on locomotor activity itself.

Flies carrying a deficiency that includes the *Nf1* locus [*Df(3R)Esp13*] over each of the *Nf1* alleles yielded similar results (Table 1), with a small number carrying the *Nf1<sup>P1</sup>* allele showing weak rhythms. The variability in the phenotype of each of the two alleles when tested individually or with the deletion suggests that the two alleles are equally affected. Expression of an *Nf1* transgene in both the *Nf1<sup>P1</sup>* and *Nf1<sup>P2</sup>* backgrounds restored rhythmicity in DD, as did expression of a *UAS-dNf1* transgene (11) driven by *elav-gal4* (which would result in expression of NF1 in all neurons) in *Nf1<sup>P1</sup>* flies. Restricting expression of *UAS-dNf1* to clock cells [lateral neurons (LNs)] by using *tim-gal4* or *pdf-gal4* drivers did not rescue the behavior, indicating that expres-

sion of NF1 in LNs is not sufficient for circadian activity.

To determine whether there was any effect on entrainment, *Nf1* mutants were studied in a 12-hour:12-hour light:dark (LD) cycle. The behavior of *Nf1* mutants in LD was consistent with an inability to translate signals from the clock [(Web fig. 1) (11)].

We next determined whether circadian clock function was affected by using ribonuclease (RNase) protection assays to determine whether the cycling of the clock components *per* and *tim* was perturbed in the *Nf1* background. The expression of *per* and *tim* mRNA in *Nf1* mutants was indistinguishable from that in *K33* flies (Fig. 1A).

We also assayed the bioluminescence rhythm of a TIM-luciferase reporter construct (11) in *K33*, *Nf1<sup>P1</sup>*, and *Nf1<sup>P2</sup>* flies for several days in DD. Significant circadian oscillations

were detected in all three genotypes (Fig. 1B), confirming that *Nf1* mutations do not affect *tim* cycling.

We next determined whether the molecular oscillations of PER and TIM proteins occurred in the LNs of the central brain, the site of the central circadian clock (2). As determined by immunohistochemistry (11), PER and TIM cycling in *Nf1* flies was normal in the LNs in adults [(Web fig. 2) (11)], and TIM cycling was also normal in larvae (Fig. 1C). TIM protein levels peaked at around circadian time (CT) 18, and no TIM could be detected during the subjective daytime (CT 6 to 12). Taken together, the results in Fig. 1 and Table 1 indicate that *Nf1* does not affect normal clock function at the molecular level but has a strong effect on a pathway that is downstream from the endogenous clock signal.

To test whether another circadian-related molecule, cAMP response element-binding protein (CREB) (10), might be affected, we monitored *K33*, *Nf1<sup>P1</sup>*, and *Nf1<sup>P2</sup>* flies carrying the CRE-luciferase (CRE-luc) reporter gene in a luminometer continuously in DD for up to 5 days (11). Average CRE-luc activity within flies was up to three times higher in the *Nf1* backgrounds than in *K33* [(Web fig. 3, left panels) (11)]. Consistent with previous observations, CRE-luc activity exhibited robust circadian oscillations in the *K33* flies [(Web fig. 3, right panels) (11)] and in both *Nf1* mutants but with substantially lower amplitudes. Thus, although *Nf1* is clearly downstream of the molecular clock components, its signaling lies upstream of CRE-mediated transcription and may control behavioral output from the clock.

Although earlier data (9) are consistent with reports showing that *Drosophila Nf1* acts through a cAMP-dependent pathway (3, 6) and would predict a decrease in CRE-luc activity in *Nf1* mutants because of a decrease in CREB phosphorylation by protein kinase A (PKA), our data show that CRE-luc activity was elevated in the *Nf1* mutants, suggesting that CREB may be phosphorylated by a kinase other than PKA—perhaps Rsk2, which requires MAPK activation (12, 13).

We tested the ability of an *hsPKA* transgene (3, 6) to rescue the arrhythmic mutant phenotype. The *hsPKA* transgene rescued rhythmicity in only one-third of the *Nf1<sup>P1</sup>* flies and in none of the *Nf1<sup>P2</sup>* flies [(Web table 1) (11)]. A larger number of *K33* flies were also arrhythmic, indicating a mild effect of the transgene alone. No improvement was observed when flies were raised and tested at 29°C (14). We suspected that clamping PKA activity to high levels, as may be predicted in this background, might have adverse effects on rhythmicity. *Nf1* mutants were therefore crossed into a *dunce* background, which lacks a cAMP phosphodiesterase and is thereby expected to have elevated levels of cAMP

**Table 1.** *Nf1* mutants exhibit arrhythmic activity. Period length was calculated only in flies that were considered rhythmic ( $P < 0.05$ ) (11). The last column reports the strength of the rhythm in these flies; the relative power values were calculated by fast Fourier transform (FFT).

Genotype	No. rhythmic (%)	Period length (hours)	FFT relative power
<i>K33</i>	46/48 (95.83)	23.70 ± 0.07	0.116 ± .01
<i>Nf1<sup>P1</sup></i>	0/28 (0.00)		
<i>Nf1<sup>P2</sup></i>	4/38 (10.53)	22.75 ± 0.17	0.031 ± .01
<i>Df(3R)Esp13/K33</i>	23/24 (95.83)	23.24 ± 0.07	0.201 ± .01
<i>Df(3R)Esp13/Nf1<sup>P1</sup></i>	5/22 (22.73)	23.40 ± 1.07	0.040 ± .01
<i>Df(3R)Esp13/Nf1<sup>P2</sup></i>	2/30 (6.67)	22.75	0.053
<i>p[w+;hsNf1];K33</i>	15/18 (83.33)	23.10 ± 0.11	0.073 ± .09
<i>p[w+;hsNf1];Nf1<sup>P1</sup></i>	18/42 (42.86)	23.83 ± 0.22	0.060 ± .01
<i>p[w+;hsNf1];Nf1<sup>P2</sup></i>	25/35 (71.43)	23.02 ± 0.09	0.050 ± .00
<i>UAS-dNf1;Nf1<sup>P1</sup></i>	7/35 (20.00)	22.43 ± 0.38	0.034 ± .01
<i>elav<sup>c155</sup>;+;Nf1<sup>P1</sup></i>	0/19 (0.00)		
<i>elav<sup>c155</sup>;UAS-dNf1;Nf1<sup>P1</sup></i>	11/13 (84.62)	23.00 ± 0.10	0.100 ± .02
<i>pdf-gal4;Nf1<sup>P1</sup></i>	4/15 (26.67)	24.5 ± 0.00	0.104 ± .02
<i>pdf-gal4/UAS-dNf1;Nf1<sup>P1</sup></i>	0/23 (0.00)		
<i>tim-gal4;Nf1<sup>P1</sup></i>	4/21 (19.05)	23.50 ± 0.62	0.052 ± .01
<i>tim-gal4/UAS-dNf1;Nf1<sup>P1</sup></i>	0/27 (0.00)		

**Table 2.** Effects of Ras/MAPK mutants on activity rhythms in *Nf1* mutants.

Genotype	No. rhythmic (%)	Period length (hours)	FFT relative power
<b>Gain of function</b>			
<i>GAP1<sup>A13P</sup>;K33</i>	19/20 (95.00)	24.76 ± 0.06	0.089 ± .01
<i>GAP1<sup>A13P</sup>;Nf1<sup>P1</sup></i>	2/17 (11.76)	24.50	0.052
<i>GAP1<sup>A13P</sup>;Nf1<sup>P2</sup></i>	0/24 (0.00)		
<i>hsRaf<sup>*M7</sup>;K33</i>	29/29 (100.0)	23.57 ± 0.09	0.115 ± .01
<i>hsRaf<sup>*M7</sup>;Nf1<sup>P1</sup></i>	0/26 (0.00)		
<i>SOS<sup>jc2</sup>;K33</i>	34/37 (91.89)	23.25 ± 0.38	0.147 ± .01
<i>SOS<sup>jc2</sup>;Nf1<sup>P1</sup></i>	9/30 (30.00)	23.00 ± 0.13	0.078 ± .02
<b>Loss of function</b>			
<i>Ras1<sup>etB</sup>;K33</i>	20/20 (100.00)	23.80 ± 0.09	0.088 ± .01
<i>Ras1<sup>etB</sup>;Nf1<sup>P1</sup></i>	18/32 (56.25)	23.25 ± 0.07	0.092 ± .02
<i>Ras1<sup>etB</sup>;Nf1<sup>P2</sup></i>	13/31 (41.94)	23.08 ± 0.18	0.097 ± .02
<i>SOS<sup>e2H</sup>;K33</i>	27/31 (87.10)	23.13 ± 0.08	0.204 ± .01
<i>SOS<sup>e2H</sup>;Nf1<sup>P1</sup></i>	18/30 (60.00)	23.14 ± 0.07	0.090 ± .01
<i>SOS<sup>e2H</sup>;Nf1<sup>P2</sup></i>	15/26 (57.69)	23.43 ± 0.19	0.084 ± .02
<i>r1<sup>x162</sup>;K33</i>	21/23 (91.30)	24.07 ± 0.10	0.053 ± .01
<i>r1<sup>x162</sup>;Nf1<sup>P2</sup></i>	15/32 (46.88)	23.27 ± 0.13	0.050 ± .01

REPORTS

(8). Both *Nf1* and *K33* flies were tested with two different *dnc* alleles: *dnc<sup>l</sup>*, which is a hypomorph, and *dnc<sup>ML</sup>*, which is a null. Although both *dnc* alleles rescued the size phenotype of the *Nf1* flies, they did not rescue the circadian phenotype. Some lethality was associated with the double mutants carrying the *ML* allele, but no effects of *dnc* on *Nf1* rhythms were noted in the few flies that survived the locomotor assay. These data suggest that the effects of *Nf1* on circadian behavior are not mediated entirely through a cAMP-dependent mechanism.

In contrast, we found that loss-of-function mutations in Ras/MAPK signaling could rescue circadian rhythms of locomotor activity. Three different mutations in the Ras/MAPK signaling pathway were crossed into the *K33* and *Nf1* backgrounds. *SOS<sup>e2H</sup>* (*son-of-sevenless*), a loss-of-function allele of a guanine nucleotide exchange factor, an activator of Ras, was the most effective, with up to 60% rescue in the *Nf1<sup>P1</sup>* flies. *Ras1<sup>e1B</sup>* is a loss-of-function mutation in a Ras protein, and *rl<sup>x162</sup>* is a loss-of-function mutation in the *rolled* protein, the *Drosophila* homolog of MAPK (Table 2). On the other hand, crossing the *Nf1* mutations into mutant backgrounds that are predicted to have the same effect as loss of the *Nf1* protein (that is, up-regulate Ras/MAPK signaling) did not restore behavioral rhythms. *Gap1<sup>A13P</sup>* flies, which are mutant for another *Drosophila* Ras-GTPase, had no significant effect nor did expression of a heat-shock inducible transgene, *hsRaf<sup>\*M7</sup>*. *SOS<sup>ic2</sup>* is thought to be a gain-of-function allele because it suppresses the *sevenless* phenotype, probably because of an overactive product (15, 16). Because the *SOS<sup>ic2</sup>* mutation has not been characterized at the molecular or biochemical level, it is difficult to derive an explanation for the proportion of *Nf1* flies that were rhythmic.

Taken together, our data indicate that circadian rhythmicity is affected in *Nf1* mutants via a Ras/MAPK-dependent signaling mechanism. However, we cannot completely rule out a cAMP-dependent aspect, based on the observation that the *hsPKA* transgene restores rhythms in one-third of the *Nf1<sup>P1</sup>* mutants, perhaps due to an inhibitory effect of PKA signaling on the Ras/MAPK pathway (17, 18).

To further address the role of *Nf1* in MAPK signaling, we determined the effects of the *Nf1* mutations on the levels of activated or phosphorylated MAPK (phospho-MAPK) (11). On average, the phospho-MAPK signal level was approximately threefold higher in the *Nf1* mutants than in *K33* (Fig. 2A). When the mutants were compared with those carrying an *Nf1* transgene driven by a heat-shock promoter, the phospho-MAPK levels were reduced, although not completely restored (Fig. 2B). Additionally, total MAPK protein

expression in *Nf1<sup>P2</sup>* flies, in particular, was lower than that in *K33*, suggesting a compensatory feedback mechanism. A similar mechanism may also account for the higher phospho-MAPK levels in *K33* flies carrying *hsNf1* (19, 20).

Because *Nf1*/MAPK signaling appeared to be downstream of the clock, we also investigated whether activated MAPK was affected in mutants lacking various clock genes. Phospho-MAPK expression was measured in *per<sup>0</sup>*, *tim<sup>0</sup>*, and *pdf<sup>0</sup>* mutants and compared

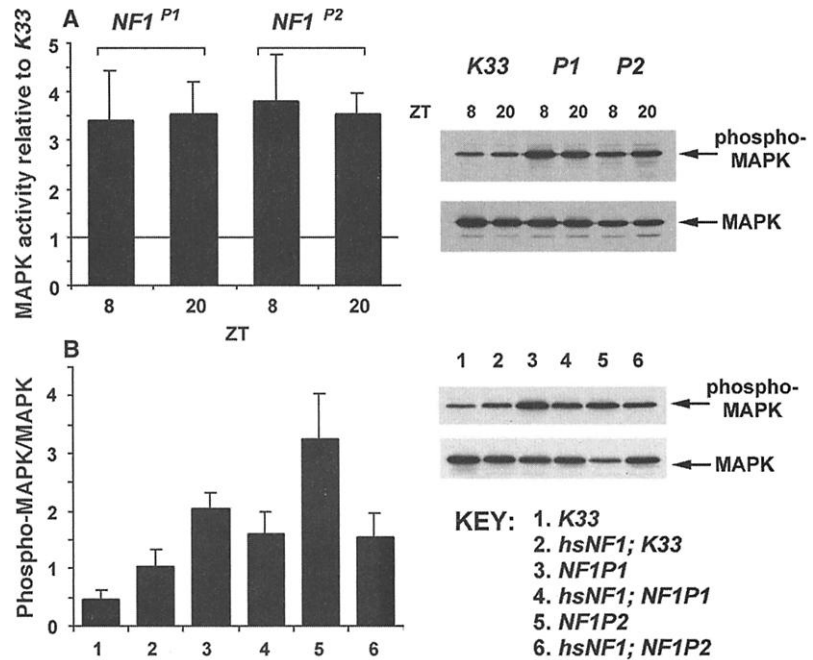
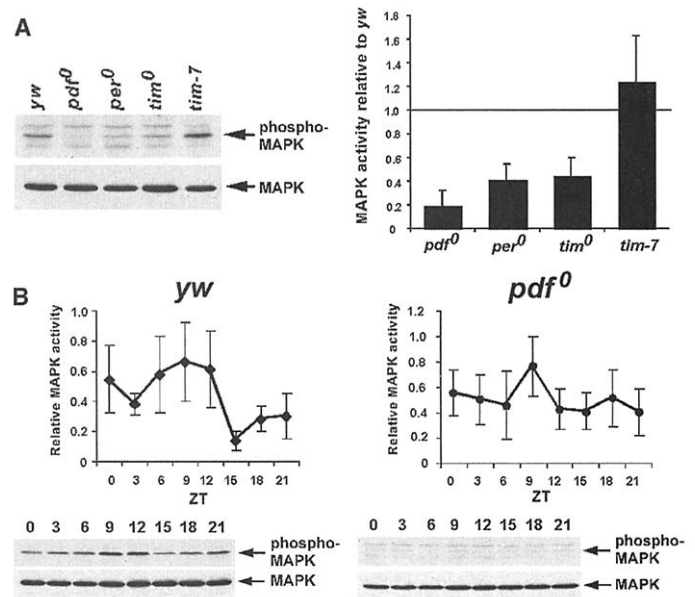


**Fig. 2.** Phospho-MAPK expression is increased in *Nf1* mutant flies. (A) *Nf1<sup>P1</sup>*, *Nf1<sup>P2</sup>*, and *K33* flies were collected at ZT 8 and 20 (8 and 20 hours after lights on, respectively) in a 12:12 LD cycle. Phospho-MAPK/MAPK density values were normalized to those in *K33* (horizontal line). Means  $\pm$  SEM from three experiments are plotted on the left (11). A representative blot is shown on the right, probed with the phospho-MAPK antibody (top) and probed again with a MAPK antibody recognizing all forms of MAPK (bottom). (B) Phospho-MAPK is reduced in *Nf1* flies expressing a heat-shock-inducible *Nf1* transgene. Values along the y axis are the phospho-MAPK/MAPK density values (means  $\pm$  SEM) from three separate experiments. A representative blot is shown on the right. The amount of activated protein in *Nf1* always exceeded that in *K33*.

**Fig. 3.** Effects of clock genes on phospho-MAPK. (A) (Right panel) Data for each genotype were plotted relative to *yw* (horizontal line); see text for explanation of genotypes. Means  $\pm$  SEM for *pdf<sup>0</sup>* and *per<sup>0</sup>* flies represent three independent experiments; those for *tim<sup>0</sup>* and *tim-7* represent five and four replicates, respectively. A representative Western blot is shown in the left panel. (B) Diurnal variations of phospho-MAPK. Relative levels of phospho-MAPK were plotted every 3 hours in a 12:12 LD cycle (ZT 0 = lights on; ZT 12 = lights off) for *yw* (left) and *pdf<sup>0</sup>* (right) flies. Means  $\pm$  SEM for each data point represent three experiments. Representative blots are shown below each graph.



## REPORTS

with the background control strain, *yellow-white* (*yw*). Phospho-MAPK was markedly reduced in all of the clock mutants, particularly in *pdf<sup>0</sup>* (Fig. 3A). Additionally, phospho-MAPK levels were restored in *tim<sup>0</sup>* mutants carrying a full-length *tim* transgene (*tim-7*). This particular transgene restores the behavioral rhythm as well in up to 75% of flies (21). Taken together with the observations described above, these data indicate that MAPK activity is a crucial component of a circadian output pathway and that its normal regulation is required for maintaining circadian rhythmicity of behavior.

To test whether MAPK activity is regulated in a circadian manner, we measured phospho-MAPK levels in *K33*, *yw*, *Nf1<sup>P2</sup>*, and *pdf<sup>0</sup>* flies in an LD cycle. Phospho-MAPK was, in general, higher during the day than during the night (in all but the *pdf<sup>0</sup>* flies), but there was no significant effect of time as determined by analysis of

variance (ANOVA) [*K33* and *Nf1<sup>P2</sup>* (14); *yw* and *pdf<sup>0</sup>*, Fig. 3B]. The lack of high-amplitude phospho-MAPK cycling on Western blots could be because it occurs in restricted regions of the brain. Alternatively, high-amplitude oscillations may not be required for rhythmic behavior—the amplitude of PDF cycling reported in *yw* nerve terminals was also low (22).

In order to determine the distribution of phospho-MAPK relative to the clock cells, immunohistochemical staining was performed on adult flies collected at Zeitgeber time 8 (ZT 8). Phospho-MAPK staining was particularly strong in the vicinity of PDF-positive nerve terminals (Fig. 4). These regions included the optic lobes [OLs (Fig. 4, A through C)] and the immediate vicinity of centrally projecting PDF neurons in the dorsal protocerebrum, suggesting that PDF receptors couple to this signaling pathway.

Brains of both *yw* and *pdf<sup>0</sup>* flies were scored

blind for phospho-MAPK staining intensity in various regions: the outer OL, which would include the lamina (if present) and outer medulla; and the inner OL, which included the inner medulla, lobula, and lobular plate (23). The *pdf<sup>0</sup>* brains were generally lower in staining intensity as compared with *yw* brains (Fig. 4, D through F and G). Significant differences were observed between the two groups in the outer OL and the central brain. In several cases, intense staining was observed in some areas in the *pdf<sup>0</sup>* background, indicating that other systems couple to MAPK signaling, as would be expected. Also, the PDF mutation is not expected to significantly affect phospho-MAPK levels during development, because the OL projections are not present in larvae.

Cyclic release of PDF in the dorsal brain is required for normal activity rhythms (22, 24), so we determined whether phospho-MAPK displayed circadian oscillations in the dorsal region (Fig. 4H). Serial sections obtained on a confocal microscope were scored blind for phospho-MAPK staining intensities (23) (Fig. 4I). ANOVA revealed a significant effect of time ( $P < 0.001$ ) on phospho-MAPK expression. Post hoc comparison with the Scheffe test revealed a significant increase at ZT 20 but no differences between ZT 2, 8, and 14. This staining profile is consistent with a previous study (22) that indicated that PDF release would be highest at night and is consistent with the hypothesis that PDF activates a Ras/MAPK signaling pathway.

Previous studies have implicated MAPK in the circadian system, as it has been shown to mediate responses to light (13, 25, 26) and to oscillate in several vertebrate systems (26–28). Our data indicate a role for *Nf1* in circadian output via the Ras/MAPK signaling pathway. The observation that MAPK activity is profoundly affected in clock mutants suggests that this signaling mechanism may directly couple to the circadian system. In particular, release of the PDF peptide from LNs may affect heterotrimeric GTP-binding protein-coupled receptors which, in turn, are coupled to a Ras/MAPK signaling pathway that is regulated by neurofibromin. Our findings also establish a link between Ras/MAPK signaling and *Drosophila* neurofibromin in vivo and suggest that NF-1 patients may suffer from sleep disturbances.

### References and Notes

1. J. A. Williams, A. Sehgal, *Annu. Rev. Physiol.* **63**, 729 (2001).
2. S. C. Renn, J. H. Park, M. Rosbash, J. C. Hall, P. H. Taghert, *Cell* **99**, 791 (1999).
3. I. The et al., *Science* **276**, 791 (1997).
4. F. McCormick, *Curr. Opin. Genet. Dev.* **5**, 51 (1995).
5. D. Viskochil, R. White, R. Cawthorn, *Annu. Rev. Neurosci.* **16**, 183 (1993).
6. H.-F. Guo, J. Tong, F. Hannan, L. Luo, Y. Zhong, *Nature* **403**, 895 (2000).
7. A. J. Silva et al., *Nature Genet.* **15**, 281 (1997).

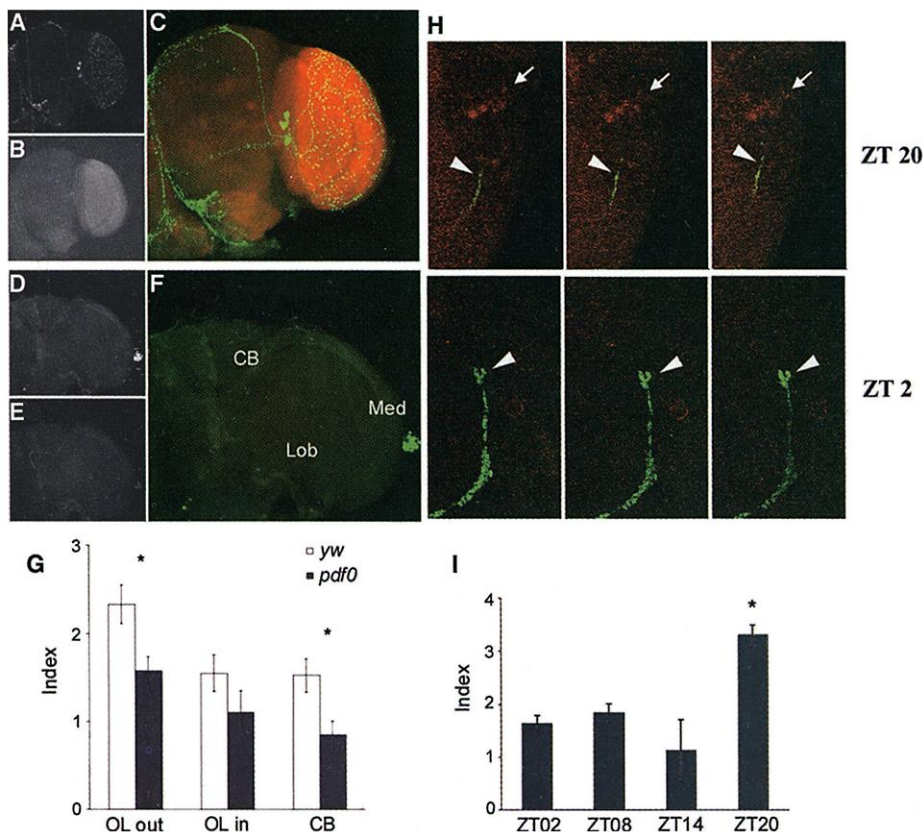


**Fig. 4.** Phospho-MAPK expression in *Drosophila* whole-mount brains. *yw* brains show LN staining of PDF (A and green in C) and OL staining of phospho-MAPK [B and red in (C)] in the region of PDF nerve terminals. *pdf<sup>0</sup>* flies (D through F) exhibit no PDF immunoreactivity [D and green in (F)] and reduced levels of phospho-MAPK [(E) and red in (F)]. CB, central brain; Lob, lobula; Med, medulla. (G) Activated MAPK [judged by scoring phospho-MAPK immunofluorescence (23)] is decreased in the OL and CB in *pdf<sup>0</sup>* flies. Asterisk denotes significance between groups as determined by Student's *t* test ( $P < 0.05$ ).  $n = 10$  flies per genotype. (H and I) Phospho-MAPK staining oscillates in the vicinity of PDF terminals in the CB. Adult *yw* flies were collected in LD at ZT 2, 8, 14, and 20 ( $n = 3, 2, 3,$  and 4 flies, respectively), and brains were processed with PDF and phospho-MAPK antibodies. (H) Representative confocal serial sections from *yw* dorsal protocerebrum for ZT 20 (top) and ZT 2 (bottom). Phospho-MAPK staining (red, arrows) was highest at ZT 20 in the vicinity of PDF terminals (green, arrowheads). (I) Scoring of phospho-MAPK staining at the terminals [as in (G)] revealed significant oscillation, with peaks at ZT 20 (asterisk indicates  $P < 0.005$ ).

8. J. D. Levine, C. I. Casey, D. D. Kalderon, F. R. Jackson, *Neuron* **13**, 967 (1994).
9. J. Majorcack, D. Kalderon, I. Ederly, *Mol. Cell Biol.* **17**, 5915 (1997).
10. M. P. Belvin, H. Zhou, J. C. Yin, *Neuron* **22**, 777 (1999).
11. Supplementary Web material is available on Science Online at [www.sciencemag.org/cgi/content/full/293/5538/2251/DC1](http://www.sciencemag.org/cgi/content/full/293/5538/2251/DC1).
12. J. Xing, D. D. Ginty, M. E. Greenberg, *Science* **273**, 959 (1996).
13. K. Obrietan, S. Impey, D. R. Storm, *Nature Neurosci.* **1**, 693 (1998).
14. J. A. Williams, A. Sehgal, data not shown.
15. R. D. Rogge, C. A. Karlovich, U. Banerjee, *Cell* **64**, 39 (1991).
16. L. Bonfini, C. A. Karlovich, C. Dasgupta, U. Banerjee, *Science* **255**, 603 (1992).
17. A. M. Huang, G. M. Rubin, *Genetics* **156**, 1219 (2000).
18. A. K. Howe, R. L. Juliano, *Nature Cell Biol.* **2**, 593 (2000).
19. A. D. Cherniack, J. K. Klarlund, M. P. Czech, *J. Biol. Chem.* **269**, 4717 (1994).
20. S. Corbalan-Garcia, S.-S. Yang, K. R. Degenhardt, D. Bar-Sagi, *Mol. Cell Biol.* **16**, 5674 (1996).
21. L. Hickman, A. Sehgal, unpublished observations.
22. J. H. Park et al., *Proc. Natl. Acad. Sci. U.S.A.* **97**, 3608 (2000).
23. Ten brains from each condition (*yw* and *pdf<sup>0</sup>*) were presented blind to four people and scored on a scale of 0 (not present) to 3 (high intensity). For each of the raters, mean scores were calculated for each brain region. The index in Fig. 4G represents the mean values  $\pm$  SEM calculated across the four raters.
24. C. Helfrich-Förster et al., *J. Neurosci.* **20**, 3339 (2000).
25. M. Akashi, E. Nishida, *Genes Dev.* **14**, 645 (2000).
26. K. Sanada, Y. Hayashi, Y. Harada, T. Okano, Y. Fukada, *J. Neurosci.* **20**, 986 (2000).
27. Y. Harada, K. Sanada, Y. Fukuda, *J. Biol. Chem.* **275**, 37078 (2000).
28. G. Y.-P. Ko, M. L. Ko, S. E. Dryer, *Neuron* **29**, 255 (2001).
29. B. Krishnan et al., *Nature* **411**: 313 (2001).
30. We thank J. Levine, P. Funes, H. B. Dowse, and J. Hall for quantitative analyses of the bioluminescence data; L. Hickman for providing *tim-luc* flies; J. de Nooij for generating *UAS-dNFI* transgenics; W. Fu and Y.-F. Chen for technical assistance; G. Cowley for providing polymerase chain reaction primers for genotyping; B. Meyer-Bernstein, E. Myers, and S. Johnson for scoring; and P. Taghert, R. Jackson, and J. C.-P. Yin for *pdf<sup>0</sup>*, *dnc*, and *CRE-luc* flies, respectively. J.A.W. and H.S.S. are supported by an NIH training grant. Supported by an NIH grant to A.S., by grants from NIH, the American Cancer Society, and the Neurofibromatosis Foundation to J.F., and by grants from NIH and the U.S. Army Medical Research Command to A.B. A.S. is a Howard Hughes Medical Institute Associate Investigator.

4 June 2001; accepted 1 August 2001

## Triallelic Inheritance in Bardet-Biedl Syndrome, a Mendelian Recessive Disorder

Nicholas Katsanis,<sup>1</sup> Stephen J. Ansley,<sup>1</sup> Jose L. Badano,<sup>1</sup> Erica R. Eichers,<sup>1</sup> Richard Alan Lewis,<sup>1,2,3,4,5</sup> Bethan E. Hoskins,<sup>6</sup> Peter J. Scambler,<sup>6</sup> William S. Davidson,<sup>7</sup> Philip L. Beales,<sup>6</sup> James R. Lupski<sup>1,3,5\*</sup>

Bardet-Biedl syndrome (BBS) is a genetically heterogeneous disorder characterized by multiple clinical features that include pigmentary retinal dystrophy, polydactyly, obesity, developmental delay, and renal defects. BBS is considered an autosomal recessive disorder, and recent positional cloning efforts have identified two *BBS* genes (*BBS2* and *BBS6*). We screened our cohort of 163 BBS families for mutations in both *BBS2* and *BBS6* and report the presence of three mutant alleles in affected individuals in four pedigrees. In addition, we detected unaffected individuals in two pedigrees who carry two *BBS2* mutations but not a *BBS6* mutation. We therefore propose that BBS may not be a single-gene recessive disease but a complex trait requiring three mutant alleles to manifest the phenotype. This triallelic model of disease transmission may be important in the study of both Mendelian and multifactorial disorders.

Locus heterogeneity in Mendelian disorders is the phenomenon whereby mutations in different genes result in a similar or identical clinical phenotype. In most reported instances, mutations at a single locus suffice to cause disease, although rare cases have been reported where mutations at two loci are necessary for pathogenesis (1) or exacerbate the severity of the phenotype (2, 3). BBS is a typical example of a rare, genetically heterogeneous

disorder. BBS patients manifest a complex and variable phenotype that includes pigmentary retinal dystrophy, polydactyly, central obesity, hypogonadism, learning difficulties, and renal dysplasia; additional features such as asthma and diabetes mellitus may also be present (4, 5). The segregation of the disorder in families and population isolates led to the hypothesis that the syndrome is inherited in an autosomal recessive manner. On the basis of this model, six *BBS* loci have been identified: *BBS1* on 11q13 (6), *BBS2* on 16q21 (7), *BBS3* on 3p12 (8), *BBS4* on 15q22.2-q23 (9), *BBS5* on 2q31 (10), and *BBS6* on 20p12 (11), with evidence for at least one more locus (12). Two *BBS* genes have been cloned recently: *BBS6* (11, 13), which encodes a putative chaperonin (14), and *BBS2*, which encodes a protein of unknown function (15).

During our analysis of *BBS6* in 163 patients, we identified eight pedigrees with

mutations. A high frequency of these (seven of eight) harbored only a single mutant *BBS6* allele (12). Furthermore, we described one consanguineous pedigree in which both the affected and unaffected sibs carried a heterozygous A242S mutation in *BBS6*, but the affected sib also exhibited homozygosity by descent (HBD) across the *BBS2* locus. This observation suggests either that BBS arises through multiallelic inheritance or that the A242S allele is a rare polymorphism (12).

The recent identification of *BBS2* enabled us to test the former hypothesis by screening the same cohort of BBS patients (16) for coding sequence alterations in *BBS2*, irrespective of haplotype-inferred chromosomal assignment for any given pedigree or previously obtained mutational data for *BBS6*. Upon deducing the intron-exon structure of *BBS2* (17), we designed suitable primers and amplified and sequenced each of the 17 exons of this gene in our entire patient cohort (18).

We identified numerous sequence alterations. In 19 unrelated patients (Table 1), the alterations fulfilled our minimal criteria for mutations, in that they caused a nonconservative amino acid change and that they were not found in a minimum of 192 control chromosomes from ethnically matched samples (19). Initial segregation analyses confirmed that *BBS2* mutations were likely to be pathogenic. We identified six pedigrees (AR171, PB005, PB020, PB026, PB058, and K059) in which two independent mutations segregated with the disease (Table 1) (20). However, despite complete DNA sequence coverage of the *BBS2* open reading frame (ORF) and exon-intron boundaries, we identified only a single mutant allele in eight pedigrees. We considered four possible explanations for this result: (i) the single alleles found may not be pathogenic but rare polymorphisms, (ii) by chance alone, we were detecting rare *BBS2* carriers, (iii) the second mutation might reside in the regulatory regions or introns of *BBS2* or might be undetectable by sequenc-

<sup>1</sup>Departments of Molecular and Human Genetics, <sup>2</sup>Ophthalmology, <sup>3</sup>Pediatrics, <sup>4</sup>Medicine, <sup>5</sup>The Texas Children's Hospital, Baylor College of Medicine, One Baylor Plaza, Houston, TX 77030, USA. <sup>6</sup>Molecular Medicine Unit, Institute of Child Health, University College London, London WC1N 1EH, UK. <sup>7</sup>Department of Molecular Biology and Biochemistry, Simon Fraser University, Burnaby, British Columbia, V5A 1S6, Canada.

\*To whom correspondence should be addressed. E-mail [jlupski@bcm.tmc.edu](mailto:jlupski@bcm.tmc.edu)